NRIAG JOURNAL OF ASTRONOMY AND GEOPHYSICS
2022, VOL. 11, NO. 1, 177–192
https://doi.org/10.1080/20909977.2022.2057147

Aeromagnetic Mapping and Radioelement Influence on Mineralogical Composition of Mesothermal Gold Deposit in Part of Ilesha Schist Belt, Southwestern Nigeria

Kazeem Oladimeji Olomo[a], Sunday Bayode[b], Olufemi Adigun Alagbe[b], Gbenga Moses Olayanju[b] and Oluwatoyin Khadijat Olaleye[b]

[a]Department of Earth Sciences, Adekunle Ajasin University, Akungba-Akoko, Nigeria; [b]Department of Applied Geophysics, Federal University of Technology, Akure, Nigeria

ABSTRACT

Airborne magnetic and radiometry data sets over potential gold mineralisation associated with mesothermal alteration zones in the western Ilesha schist belt, Southwestern Nigeria, were interpreted. This was done to provide information on possible extent of geologic transformations that accompanied gold mineralisation in the area. Interpreted gamma spectrometric data were successfully used in delineating zones of hydrothermal alteration associated with potassium K enrichment as the target for gold deposits. The geological structural features that host the ore deposits were identified as lineament represented by lithological contacts and faults/fractures that were successfully exacted from the airborne magnetic data. The potassium deviation (KD) map was computed to enhance the potassium signature of rocks in the area of study. Thus, the KD map represents real potassium distribution across the study area emanated from hydrothermal alteration where hydrothermalised zones were displayed by high KD values. First vertical derivative (FVD) and total horizontal gradient (THG) maps were used to delineate lineaments. These lineaments were connected using the frequency rose diagram with two main lineament set,; major and minor lineaments observed. The 3D Euler deconvolution (EUD) method was also applied on the THG map to locate and evaluate depths to subsurface structures. The best 3D EUD solution for dykes and contacts modelled using the Structural Index of zero (S.I = 0) was used to estimate the depth to these anomaly sources at 300 to 700 m in the study area. The EUD results also revealed several subsurface structures which were hidden in the existing geological map of the study area. A prospective mineralisation map was produced from the synthesis of both magnetic lineaments and alteration zones maps derived for the study area, showing the areas of probable high mineral resources. Strong relationships were observed between the mapped hydrothermal altered zoneseologic structures and superimpose known gold mining pits.

ARTICLE HISTORY
Received 11 January 2022
Revised 28 February 2022
Accepted 18 March 2022

KEYWORDS
Potassium deviation; 3-D Euler deconvolution; hydrothermal alteration; aeromagnetic enhancement; mineralisation

1. Introduction

The studied area is among the most important schist belts in Nigeria. It has attracted a lot of interest due to its significant mineral resources such as gold and sulphide. It has been surveyed and studied extensively by several geoscientists for many decades in the context of geological mapping, geochemistry, structural geology and geophysical survey. Several authors have revealed in their series of papers that the area is highly mineralised Odeyemi 1993; Kayode, 2009; Onyedim and Ocan, 2009; Ariyibi 2011; Oyinloye 2011; Kolawole and Anifowose 2011; Adelusi, *et al*., 2013; Akinlalu et al. 2018). The belt is believed to subsist numerous occurrences of mesothermal minerals, especially primary and alluvial gold deposits. These minerals are primarily hosted in quartz veins, which occur along different lithologies. These veins include fine grained mica schists, amphibolite schists and different form of gneisses (Akande and Fakorede, 1988; Ariyibi 2011; Oyinloye 2011). Geochemical analyses of rocks hosting gold deposits revealed that Cu, Zn and Pb enrich the altered rocks (Oyinloye 2011). In addition, the area is enriched with heavy rare earth elements such as chalcopyrite, sphalerite and galena which reflect the presence of sulphide deposits (Oyinloye 2011). The concentration of potassium oxide (K_2O) in biotite granite gneiss is evidence of rich potassium (K) bearing rock forming silicates (Ariyibi 2011). The geochemical data from the study area also show elemental association of Fe–Mn, Pb–Cr, and Cd–Zn (Elueze 1986).

In a bid to investigate mineralisation potentials of the study area, previous geophysical research did not target geophysical signatures of hydrothermal alteration zones. Previous authors, Ako (1980), including Folami and Ojo (1991), Folami (1992), Adelusi *et al.* (2009), Adelusi, *et al.* (2013) Akinlalu *et al.* (2016) and (Akinlalu et al. 2018), only utilised electrical and

CONTACT Kazeem Oladimeji Olomo kazeem.olomo@aaua.edu.ng Department of Earth Sciences, Adekunle Ajasin University, Akungba-Akoko, Nigeria

magnetic methods to delineate structures and their implication on gold mineralisation. However, attempt has not been made in studying the connection between hydrothermal altered zones and existing gold deposit within the study area. This article focused on the influence of hydrothermal alteration on known the mineralogical composition of western part of Ilesha schist belt. The findings of this research pave the way for the construction of mineral predictive maps linking the lineament, chemical alteration and known gold mineralisation. In order to achieve this, the airborne geophysical dataset comprises magnetic and radiometry.

Gold mineralisation occurrence in Ilesha schist belt is associated with veins and dikes that serve as conduits for hydrothermal alterations and injections of mineralising fluid. This enables the application of the airborne magnetic method in delineating the geologic structures. The airborne magnetic method has widely been used in preliminary geological reconnaissance, investigation of shallow and deep magnetic bodies. (Korhonen 2005; Airo and Mertanen 2008; Araújo et al. 2014; Oskooi and Abedi 2015). Airborne radiometry provides important information about areas with a great influence of hydrothermal alteration as a result of distribution contents of the radioactive elements K, eU and eTh in rocks (Minty 1997; Tourlière et al. 2003; Ferreira et al. 2014; Ribeiro and Mantovani 2016).

2. Geologic setting and mineral occurrence

The study area is located in Ilesha, southwestern part of Nigeria (Figure 1), and covers a land expanse of 600 square kilometres (20 × 30) $Km^{2.}$ The study area covers longitude 4° 37' E to 4° 55' E and latitude 7° 30' N to 7° 41' N. It lies primarily within the Ilesha Schist Belt (Ajibade 1982; Odeyemi 1993; Okonkwo et al. 2014; Adeoti and Okonkwo 2017) of the crystalline Basement Complex, Southwestern Nigeria. The lithological units include the migmatite gneiss complex of the surficial Quaternary which is the oldest rock type, quartz schist, quartzite, amphibolite schist, granite gneiss (biotite-hornblende-gneiss and biotite-hornblende-granite), amphibolite (the youngest rock type of the study area) (Figure 2) and alluvial deposit (Burke et al. 1976). The gneissic complex is made up of undifferentiated paragneisses and orthogneisses (Oyinloye 2011). The orthogneisses are usually located below the quartzite schist and are associated with circular/rounded tops, which are very poor in vegetation and underlain topographic highs (Oyinloye 2007). Different degrees of metamorphosis have taken place within the orthogneisses (Rahaman and Ocan 1978; Oyinloye 2004a, 2006b, 2007). The orthogneisses are interconnected by quartz-feldspar pegmatoids of various proportions, and the foliation varies between weak and medium intensities (Ajibade and Fitches 1988). The texture and nature of the orthogneisses is granitic (Obaje 2009), and the undifferentiated gneisses are located at the lower base of steep valleys, often found between quartzite ridges (Okonkwo et al. 2014). Structurally, the study area comprises fractures,

joints, regional and minor faults. These structures trend predominantly in the NE-SW direction. This trend is the result of Pan African Orogeny involving collision between the West African Craton and the Pan African mobile terrain (Ajibade 1982).

Fracturing, shearing and alteration are the regional and local controls of gold mineralisation in the study area, exceptionally made up of a system of transcurrent and subsidiary faults, and other structures with associated Pan African age (Ho and Groves 1987). This regional fault system has been proven to be a characteristic of mesothermal gold deposit worldwide (McCurry 1976; Matheis and Caen-Vachette 1983; Kuster 1987; Matheis, 1990; Maurin and Lancelot 1990; Ekwueme and Matheis 1995). Gold mineralisation as blebs, flakes and native grains occurs together with pyrite (Oyinloye 2002b) in hydrothermal alteration zones, fractures, joints and minor faults. The gold mineralisation spatial relationship with trans-crustal lineaments is a probable implication that the gold deposits are related to convergent margin tectonics (Murat 1972; McCurry and And. Wright 1972; McDonald 1986). These mineralised lodes are made up of silicified fine-grained foliated biotite gneiss typically invaded by both discordant and concordant pegmatitic quartz-feldspar veins (Ajibade 1979, 1982; Odeyemi 1993; Anifowose and Borode 2007; Ariyibi 2011 ; Oyinloye 2011; Ademeso et al. 2013; Okonkwo et al. 2014; Adeoti and Okonkwo 2017; Akinlalu et al. 2018). The connections of the lineaments with magmatic bodies' couple with their extensive length (less than 100 km) suggest that they are trans-crustal structures extending into the lower crust and mantle (Maurin and Lancelot 1990). These have generated a single extended zone of gold mineralisation hosted by a shear zone now represented by chlorite and calcite alteration, in addition with quartz veining and pyrite formation. Observation from cursory examination suggests that most gold-associated sulphides in the study area do not contain pyrrhotite, which according to Burke et al. (1976), these could be as a result of the late episode of mineralisation or remobilisation of sulphide. Gold mineralisation is visible both in the altered wall rock of biotite granite gneiss and quartz-feldspar veins (Elueze 1986; Oyinloye 2011) within the area. Elueze (1986) reported that native gold occurs alongside with a silver-gold telluride called petzite within the quartz veins and pyrite. The native gold blebs have a size of about 10 microns (Segilola Technical report 2016). The mineralised zone

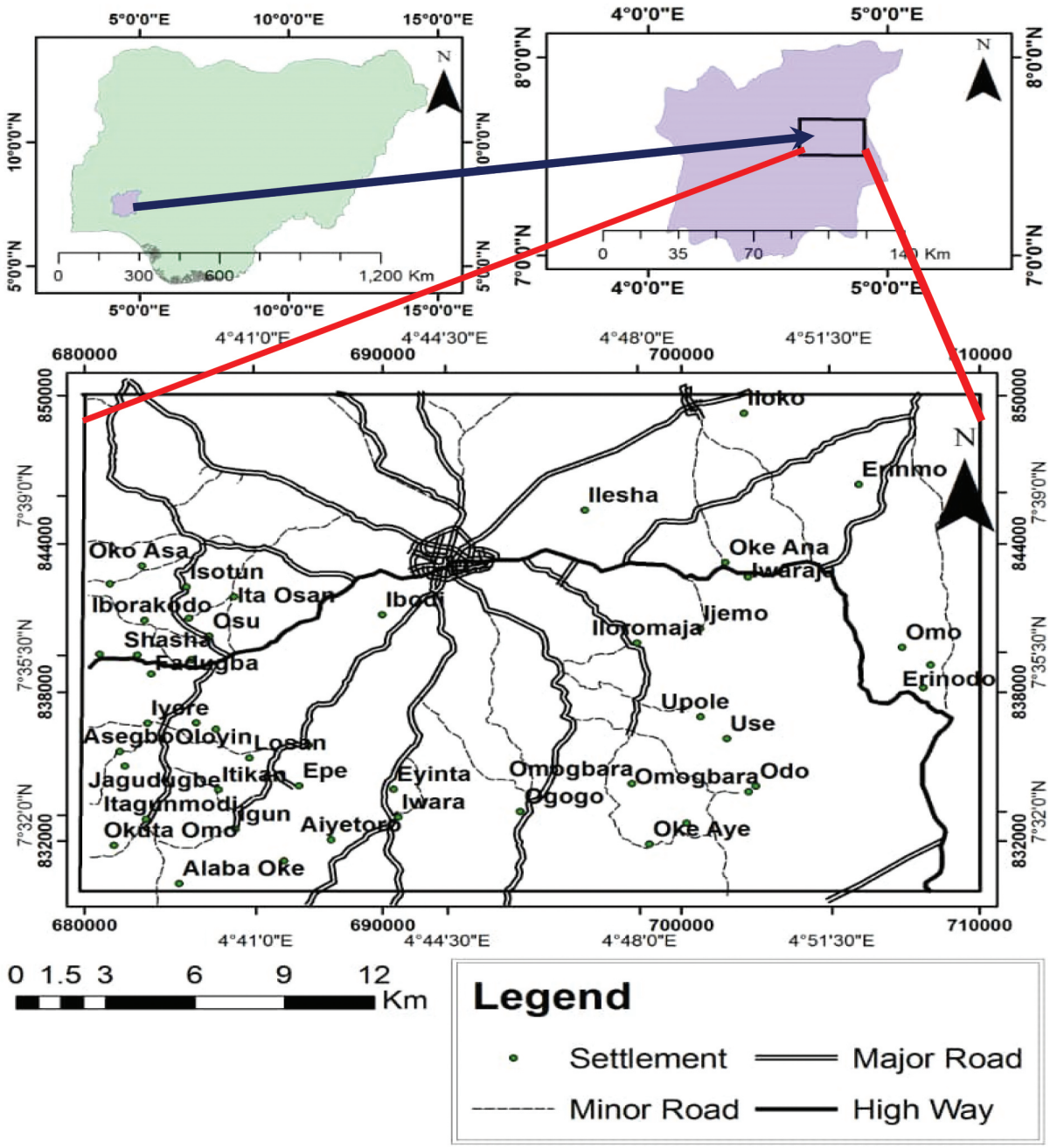

Figure 1. Base map of the study area (Insets; map of Nigeria and Osun State, modified after FSN (Federal Survey of Nigeria) 1964).

in the study area forms essentially a single elongate body varying between 2 m and 20 m thick, 2 km in strike and 70 to 200 m in depth (Segilola Technical report 2016).

3. Material and methods

Geophysical data employed include airborne magnetic and radiometry. Aeromagnetic data in excel format acquired through 7 Cessna Caravan fixed-wing aircrafts equipped with 3x Scintrex CS3 Caesium Vapour magnetometer and Flux-Adjusting Surface Data Assimilation System for data acquisition and magnetic counter, respectively, were provided by Nigerian Geological Survey Agency (NGSA). Also, a high-resolution airborne radiometric data were gotten from the Nigerian Geological Survey Agency (NGSA). It was acquired using 512-channels gamma-ray spectrometers (NaI "Tl" crystal size of 2″ × 2″) attached to fixed-wing aircraft.

The acquisition of airborne magnetic data was performed and processed by Fugro Airborne surveys in 2009. The data were recorded along the 500-m line spacing along the NW-SE direction and a tie line spacing of 5000 m in the NE-SW direction. The aeromagnetic data were later produced as a total magnetic intensity (TMI) map in a grid cell size of the 5000 m interval using Geosoft (Oasis Montaj™) version 6.4.2 (HJ) software. Enhancement of the TMI involved removal of unwanted high-amplitude short-wavelength features using non-linear filtering. To enhance aeromagnetic anomalies and highlight more

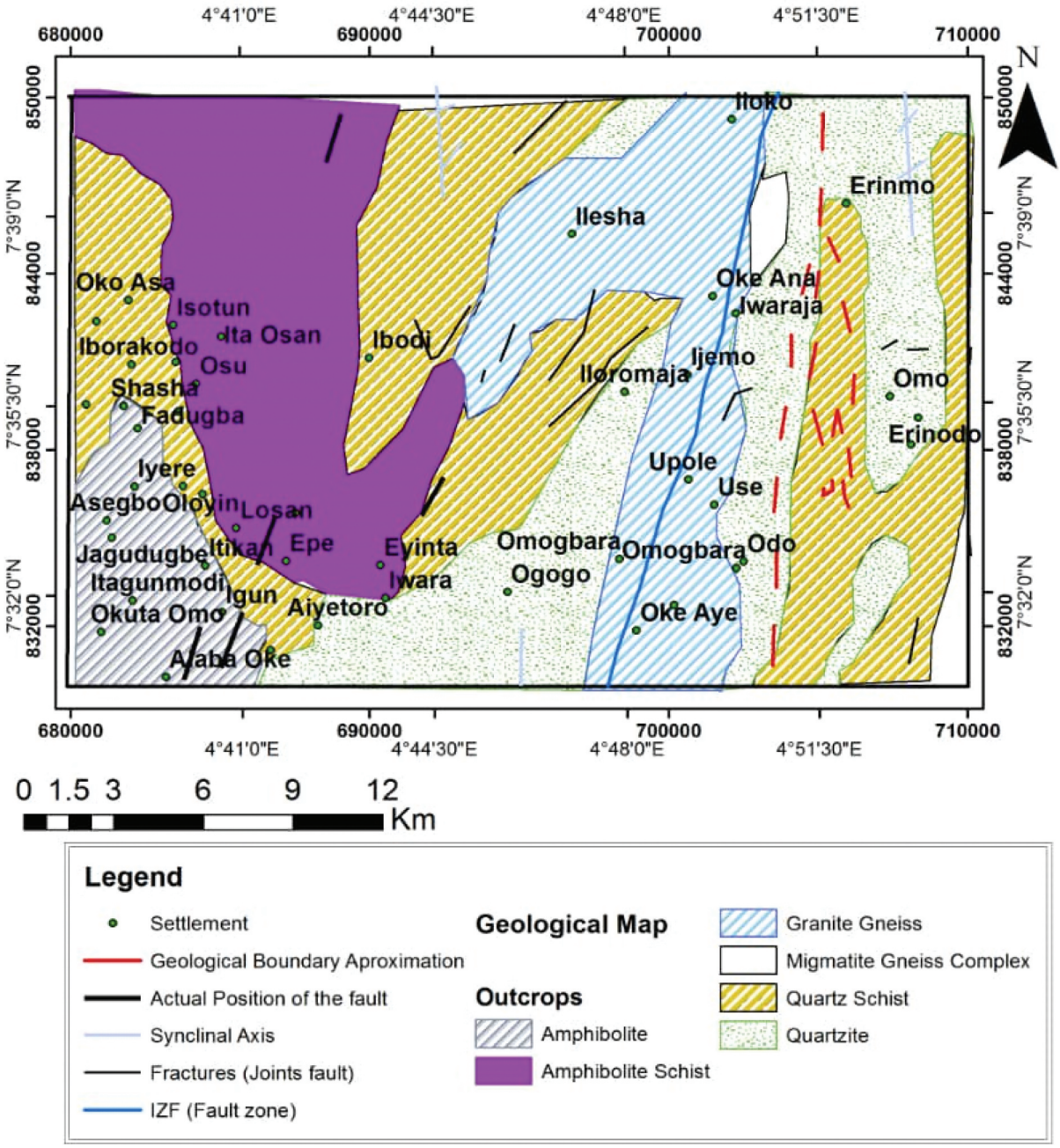

Figure 2. Map showing the geology of the study area (modified after Odeyemi 1993).

useful information, enhancement techniques such as reduction to equator (Rajagopalan 2003; Ndousa-Mbarga et al. 2012), first vertical derivation (Nabighian 1972, 1974; Miller and Singh 1994; Verduzco et al. 2004; Wijns et al. 2005; Cooper and Cowan 2006), total horizontal gradient (THG) (Cordell and Gruch 1985) and 3-D Euler deconvolution (Thompson 1982: Reid et al. 1990; Roest et al. 1992) play an important role in amplifying the lineament and structural complexity and estimate the depth and location of magnetic sources.

Application of RTE filter was based on the fact that the study area is situated in a low latitude region (between latitude 7° 30′ – 8° 00′ N), which allows the observed magnetic anomalies to be placed directly over the magnetic source bodies (Gilbert and Geldano 1985). The FVD filter enhances higher frequency resulting from shallow magnetic bodies and has the effect of removing regional trends. The FVD is useful in identifying closely spaced magnetic bodies by providing better resolution of magnetic lineament. The total horizontal gradient was generated in order to identify locations of near-vertical lithologic changes of contrasting magnetic susceptibility and also facilitate the locations of magnetic bodies in reference to depth. The Euler deconvolution of the aeromagnetic field data was carried out to determine the locations and depths of the magnetic bodies and other geologic sources in the area, using the optimum structural index of 0 for the structural features in the area. The structural features, airborne magnetic lineaments and their different alignments

in the study area were deduced from the first vertical derivative and 3-D Euler deconvolution maps. These were built into ArcGIS software to generate the composite aeromagnetic lineament map of the study area. The map showing the relationship between the structural features and the hydrothermal zones in the area was generated.

The acquisition of airborne radiometry data and its processing into grids (5000 m cell size) was carried out by Fugro Airborne surveys. The Geosoft software was further used to process radioactive distribution of the primary radioelements. Studies have shown that strong potassium anomalies are related to hydrothermal alteration which is potential mineralisation zones (Galbraith and Saunders 1983; Hoover and Pierce 1990; Dickson and Scott 1997). The R–G–B band ratios, colour space and interactive contrast stretching of single bands were applied for identification and characterisation of radiometric signatures related to mineralisation, trends of structures and pattern of geologic units. In some instance, lithology can obscure recognisable radioelement signatures, most especially potassium enrichment, thus to effectively locate the areas of chemical alteration associated with potassium enrichment requires further analysis. This is necessary because the potassium signature is hampered by the similarity of signatures of different rocks type (Gunn et al. 1997; Barbuena et al. 2013). Potassium deviation (KD)was derived to correct the anomaly and amplify potassic alteration zones, resulting in genuine potassium enrichment by filtering off unwanted signature. This method was introduced by Saunders *et al.* (1987) and proposes that thorium values are used as a guide to subject lithologic under control in order to define genuine potassium values. Thorium normalisation of the data will cancel the contributions of lithology and other environment factors, including all undesired variables, on potassium concentrations. Thorium being used as a normaliser is due to its characteristics tendency of geochemically inactiveness (Adams and Gasparini 1970). To highlight the genuine potassium value (Kv) with respect to thorium concentration, (De Quadros et al. 2003) Eq. 1 was utilised in generating the potassium deviation map using Oasis Montaj™ software,

$$K_{v=KMapAveThmapave\times ThMap,} \quad (1)$$

where K_v is the ideal potassium value, K is the potassium concentration and Th is the thorium concentration.

Potassium Deviations (KD) anomalies of genuine values from ideal values are obtained by equation (2),

$$KD = K - K_vK_v. \quad (2)$$

This represents the potassium distribution and concentration resulting from hydrothermal alteration.

4. Results and discussion

4.1. Total magnetic intensity map of the study area

Figure 3 shows the total magnetic intensity map (TMI) of the study area; it provides useful and important information for the delineation of important structural architecture of the subsurface. It emphasises that the intensity and the wavelengths of local anomalies shows a magnetic intensity range of −322nT to 500nT, suggesting contrasting rock types in the basement of the study area. The

TMI is characterised by relative high magnetic intensity values (1.9 nT and 500 nT) which coincides with amphibolite schist and amphibolite on the surface geological map. The relatively low magnetic intensity values (−1.9 nT and −322 nT) are prominent on amphibiolite, granite gneiss, migmatite gneiss complex, quartz schist and quartzite.

4.2. Reduction-to-equator of magnetic anomaly

The output of the Total Magnetic Intensity map of the study area, which was reduced to the equator, is presented in Figure 4. Figure 4 is similar to the Total Magnetic Intensity (TMI) anomaly map of the study area because of the low magnetic angle of inclination (< 15°) in the study area. In a low magnetic latitude regions around the equator where the study area is situated, positive magnetic intensity values in pink colours and negative magnetic intensity values in blue colours of amplitude magnetic anomalies due to magnetic effects of different lithologies and geologic materials correspond to low and high magnetic susceptibilities, respectively (Thomas and Harris 2009). Consequently, negative magnetic intensity values are due to the magnetic anomalous body of high magnetic contents material, while positive magnetic intensity values attribute to weak magnetic material which could be geologic structures. The western part of Figure 4 comprises magnetic high characterised by amphibolite schist and quartz, schist while the eastern section is distinctive of magnetic low. The magnetic low are characteristic of granite gneiss, migmatite gneiss complex and quartzite rocks in the study area. These weakly magnetised rocks are related to metamorphosed and highly weathered migmatite rocks, which are mainly gneisses. Minimum correlation is observed between Figure 4 and geology map of the study area. This low correlation might be as a result of magnetic susceptibilities contrast of the underlying rocks, extending across the edges into another due to intense weathering and transportations of minerals across the entire area. This shows that the mesothermal gold deposits within the study area are structurally controlled, and their occurrence is not limited to a particular rock types. Fracture, fault and stretched

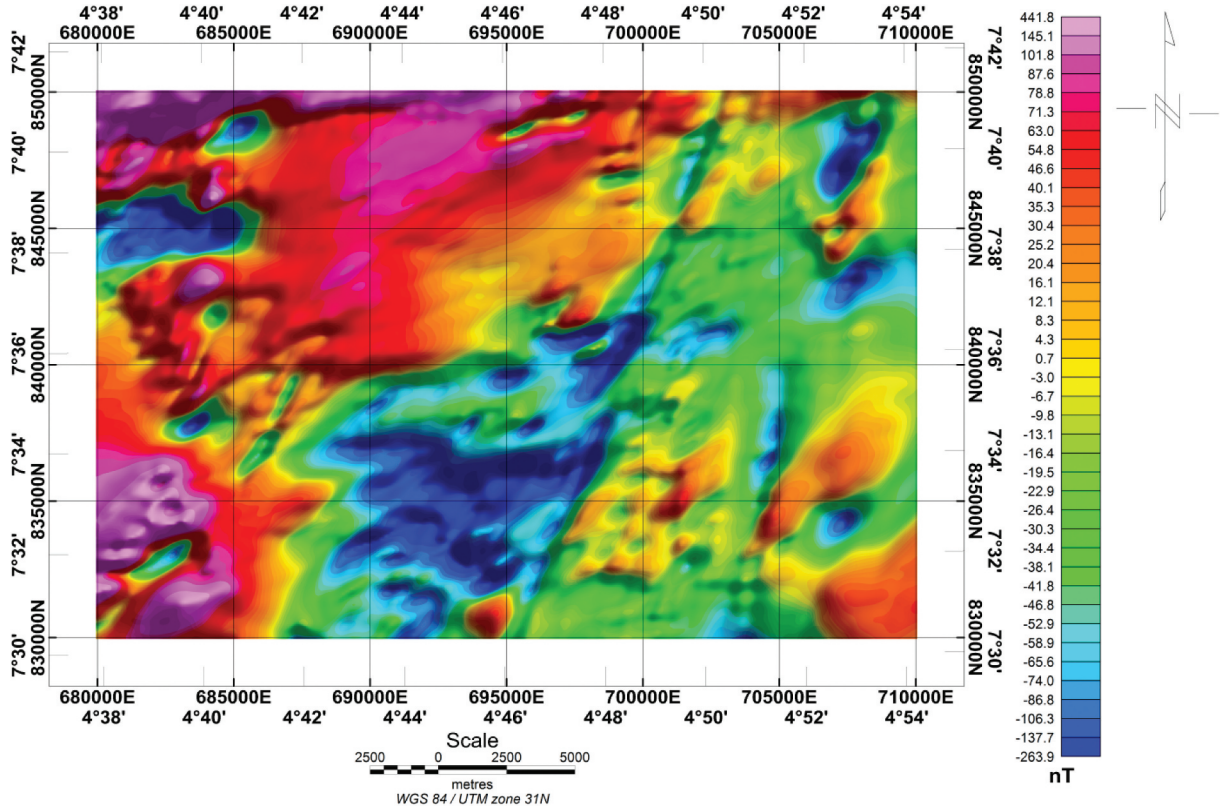

Figure 3. Total Magnetic Intensity (TMI) map of the study area.

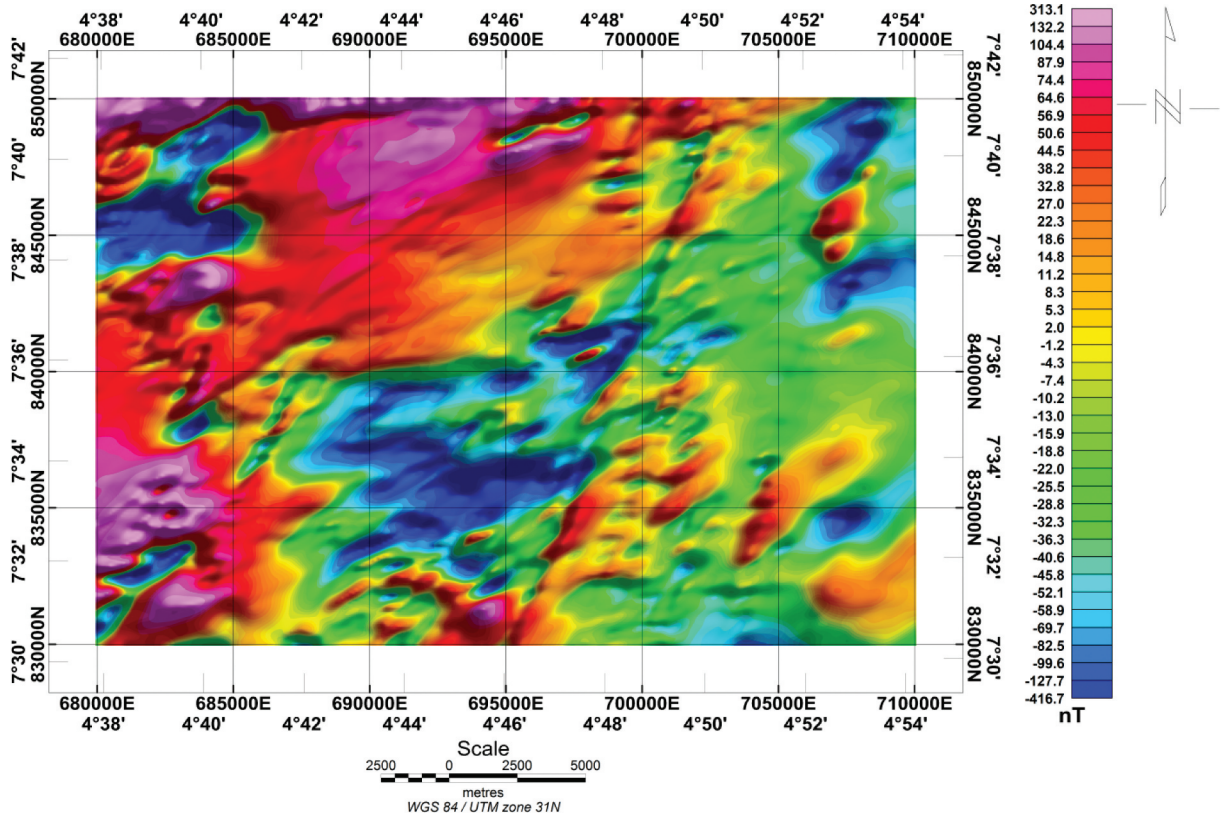

Figure 4. Reduction to the equator map of the study area.

shear zones, which play an important role as a conduit for mineralising fluid, can be expressed as linear negative anomalies on RTE map (between −1.2 nT and −417 nT). Also, according to Airo (1997), faults within the study area may also be identified as steep gradients linear belt. The imprint of these magnetic fabrics is observed on quartz schist, quartzite, granite gneiss and amphibolite on the surface geologic map. Faults with

magnetic low are as a result of depleting magnetic susceptibility due to oxidation of magnetite to haematite, along the axis of immense rise in permeability for groundwater flow. However, negative anomalies/magnetic low do not really indicate the presence of non-magnetic mineral. In a situation whereby remnant magnetisation is absent, high-low pairing implies the dipolar nature of induced magnetisation. Magnetic high is produced by the pole nearer the surface, while the deeper pole on the hand produces magnetic low (Thomas and Harris 2009). It was also observed from Figure 4, a regional lineament trend that runs diagonally from NE-SW. This is called Ifewara faults in the western part of Ilesha schist belt which form part of the structure dividing Ilesha schist belt into two. This is also observed on the geologic map of the study area.

4.3. First vertical derivative (FVD) map

Figure 5 shows a first vertical derivative map of the study area. From comparison of Figure 5 with Figure 4, structural features such as faults, fractures and folds, not visible in Figure 4, are well pronounced on Figure 5. It reflects clearly enhancement of structural features that probably serve as a major pathway for hydrothermal activity in the study area. Observation on Figure 5 revealed two types of lineaments. These lineaments can be classified as (1) major lineaments trending in the NE-SW direction and (2) minor lineaments trending in NW-SE, NNE-SSW and E-W directions. These lineaments are associated with faults, fractures, dykes, joints and veins. Gold mineralisation within this area could be as a result of the identified geological structures, which are possible sources for trapping and migration of mineralising fluid, through the concealed conduits within the earth. NNE – SSW striking lineament could represent zones of recognised quartz and pegmatite veins (De Swart 1953). The lineament has a maximum magnetic amplitude of −0.041369 nT/m sqr and a minimum of −1.578481 nT/m sqr, while the NE-SW direction represents the various tectonic episodes associated with western part of Ilesha schist belt.

4.4. Total horizontal gradient (THG)

The aim of the computation of the total horizontal gradient THG is to identify locations of near-vertical lithologic changes of varying magnetic susceptibility. Information on the magnetic field variation along the two orthogonal axes (horizontal and vertical) completely defining the anomalies is well amplified in the THG map. Consequently, structural features and boundaries of causative sources can be enhanced. Figure 6 shows the THG map of the study area in which prominent structurally trends NE-SW, NW-SE, and W-E directions were observed. Keating and Pilkington (2004) emphasised the importance of THG filter in mapping edges of magnetised bodies and thus tends to accentuate shallow anomalies. The map shows gradients ranging from 0.000076 to 1.671164

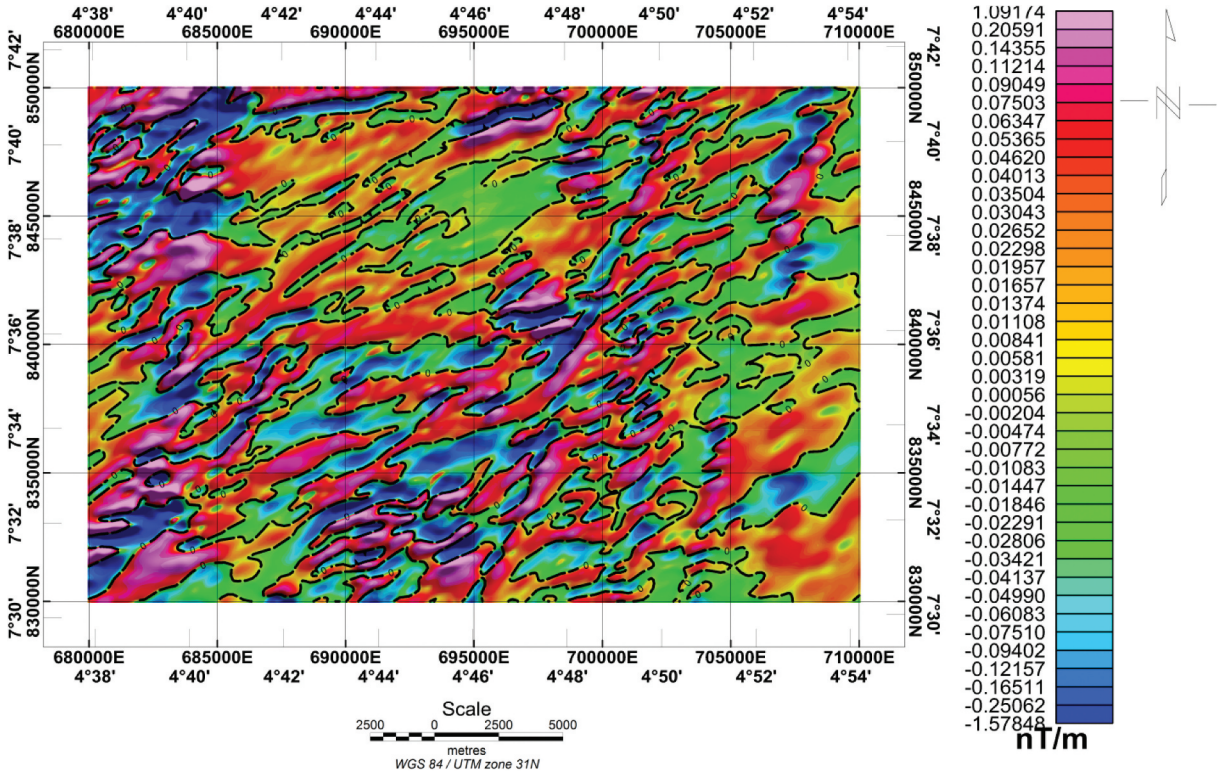

Figure 5. First Vertical Derivatives (FVD) of the study area.

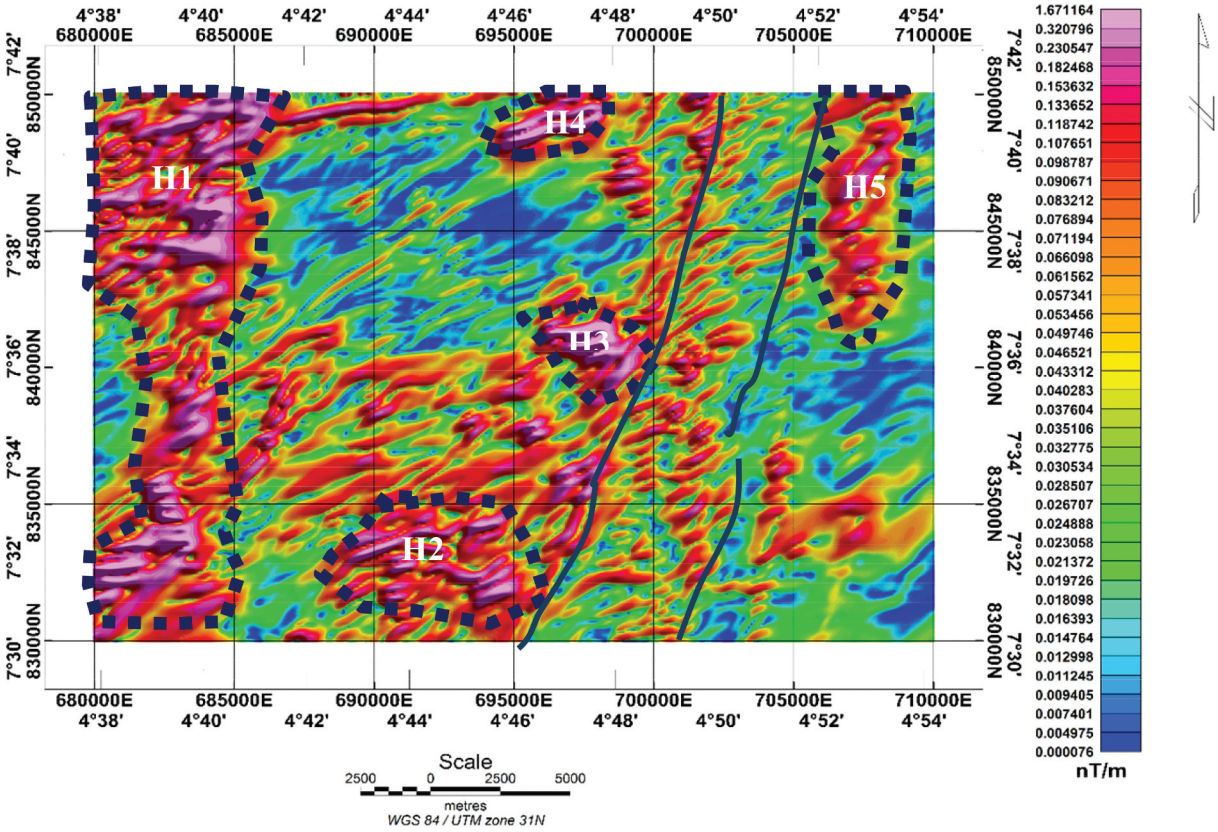

Figure 6. Total horizontal gradient map of the study area.

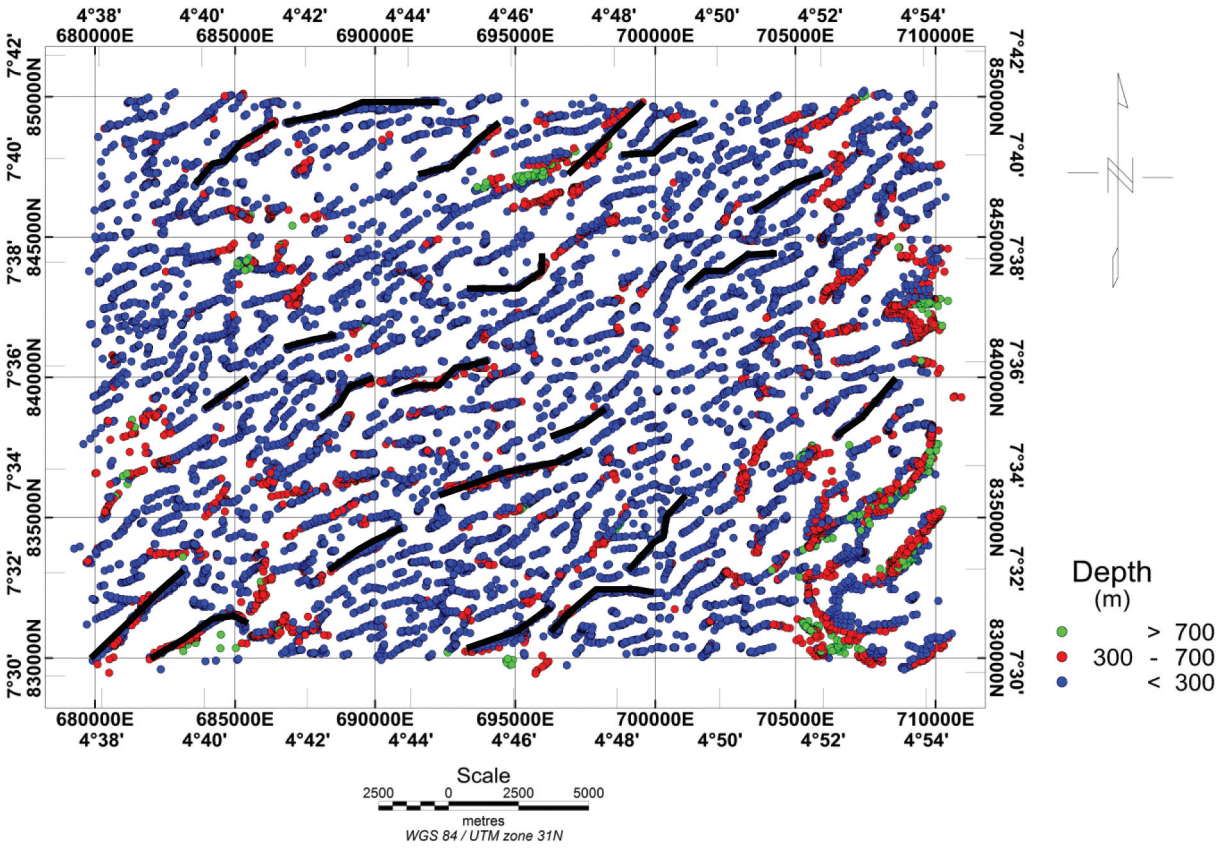

Figure.7. 3-D Euler Structural Index (SI = 0) showing interpreted structural features and their depths.

nT/m. Zones which showed peaks values on the THG map can be diagnostic of geologic structures, which provide conduit for hydrothermal alterations in the investigated area. This observation suggests a structurally controlled mineralisation within the area of study. The observed peaks are represented by H1 – H5 in Figure 6.

4.5. Depth estimate using 3-D Euler deconvolution

The locations and depths of magnetic anomaly sources and other geologic sources were determined using 3-D Euler Deconvolution (EUD) by setting an appropriate Structural Index of the source body. Trend characteristics of magnetic lineaments were highlighted using the 3-D EUD. The process was carried out using structural indices (SI) of 0 (Figure 7). Structural index is a criterion that gives detailed geometric information of magnetic causative bodies. Figure 7 reveals a characteristic cluster of diagnostic structural bodies (fractures/faults) trending predominantly in the NE-SW, while the depth range is from 300–700 m.

4.6. Composite aeromagnetic lineament map

Figure 8 shows a composite aeromagnetic lineament which was derived from FVD, THG and EUD using structural index (SI = 0) maps. Figure 8 has been scrutinised and correlated using the frequency rose diagram (azimuth-frequency) to produce Figure 9. Two main closely related lineament trends were observed in Figure 6. This relation resulted from tectonic activities giving rise to fractures, faults and dyke intrusion with the major trends in the NE-SW and E-W and minor trend in NW-SE.

4.7. Composite aeromagnetic lineament density map

Figure 10 shows an aeromagnetic lineament density map of the study area. The high-density area with Green and Red (Figure 10) reveals the potential pathway for hydrothermal alteration fluids, therefore, suggesting that structures are main control of the mineralisation in the area. The high lineament density is very prominent around granite gneiss, quartz schist and amphibolite schist. With these lineaments concentration in the area (Figure 10), high hydrothermal alteration is possible.

4.8. Potassium concentration

Analysis of potassium concentration was carried out, aiming to identify the pattern of deposition of mesothermal gold with respect to the host rocks. Mineralising hydrothermal solutions is generally enriched by the potassium element during invasion of host rocks and the most reliable guide for

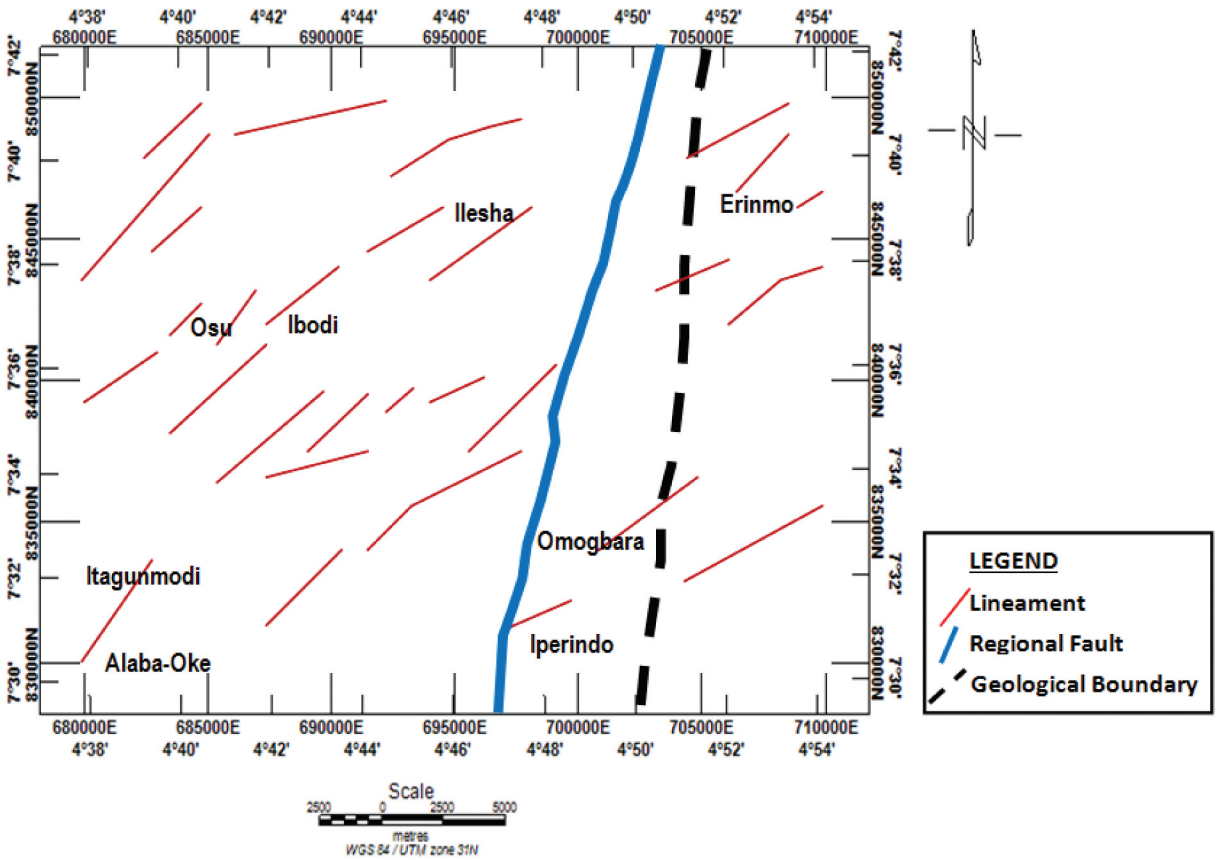

Figure 8. Integrated aeromagnetic lineament map of the study area.

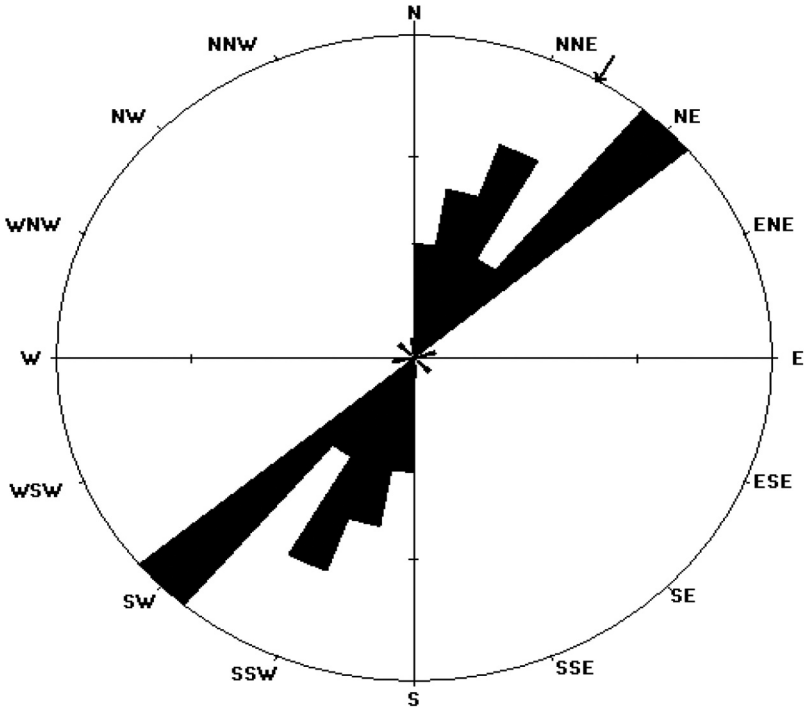

Figure 9. Rose (Azimuth-frequency) diagram of aeromagnetic lineament orientations.

mesothermal gold deposits exploration (Hoover and Pierce 1990). This method was employed to isolate hydrothermalised zones pertinent to known gold mineralisation within the area. Areas with potassium (K) high were interpreted as alteration zones. Potassium highs are recognised in the potassium concentration map (Figure 11). These potential highs are delineated within the East central and South-Eastern part of the investigated area and found to tally with amphibolites,

granite, gneiss and quartzite distinguishable by the elongated high anomalous zone (between 1.1184% and 4.4530%). Hence, the weak K signature (0.3475% – 0.1737%) is observed in the area occupied by quartzite schist, amphibolites schist and migmatite gneiss complex, except some locations with a moderate K concentration. High K anomalies denoted by H1-H5 were interpreted as hydrothermal alteration zones responsible for gold mineralisation in the study area. Good correlation is observed on high K signature values H1-H5 and the high total horizontal gradient denoted by H1-H5 on the total THG map, suggesting a perfect connection between structural features and hydrothermal alteration zones. Alteration is immense around H4, which provides an exact match with regional lineament anomaly on the integrated aeromagnetic lineament map (Figure 8) and consistent with the regional fault zone on geology map (Figure 2). This is an evidence of mesothermal gold deposits which are generally found to be associated with regional lineaments (Figures 8 and 11).

4.9. Potassium deviation (KD)

The potassium deviation KD map (Figure 12) emphasises some important targets for mineral exploration in the study area. It filters off unwanted signals caused by weathering and lithologies culminated into signatures similarity on the potassium concentration mapvand thus accentuates alteration zones. Anomalies represented by H1-H5 on the KD map are true representative of hydrothermal alteration zones devoid of aforementioned factors that have signature similarity with potassium enrichment. The KD map shows a good correlation with the potassium map (Figures. 11 and 12). Zones with

high potassium value (Figure 11) were in agreement with the high KD value except that the western part of the potassium map with moderate to low concentrations (H1 and H2) is well enhanced on the KD map.

4.10. Relationship between magnetic lineaments and alteration zones

Hydrothermal alteration zones in the study area are pronounced and more concentrated around the geological structures (shear zones and fractures) as well as boundaries between different lithological units. The alteration zones are more pronounced by correlation between potassium and KD maps. The interpreted airborne magnetic and radiometric data sets were integrated to create geologic structure and alteration zones

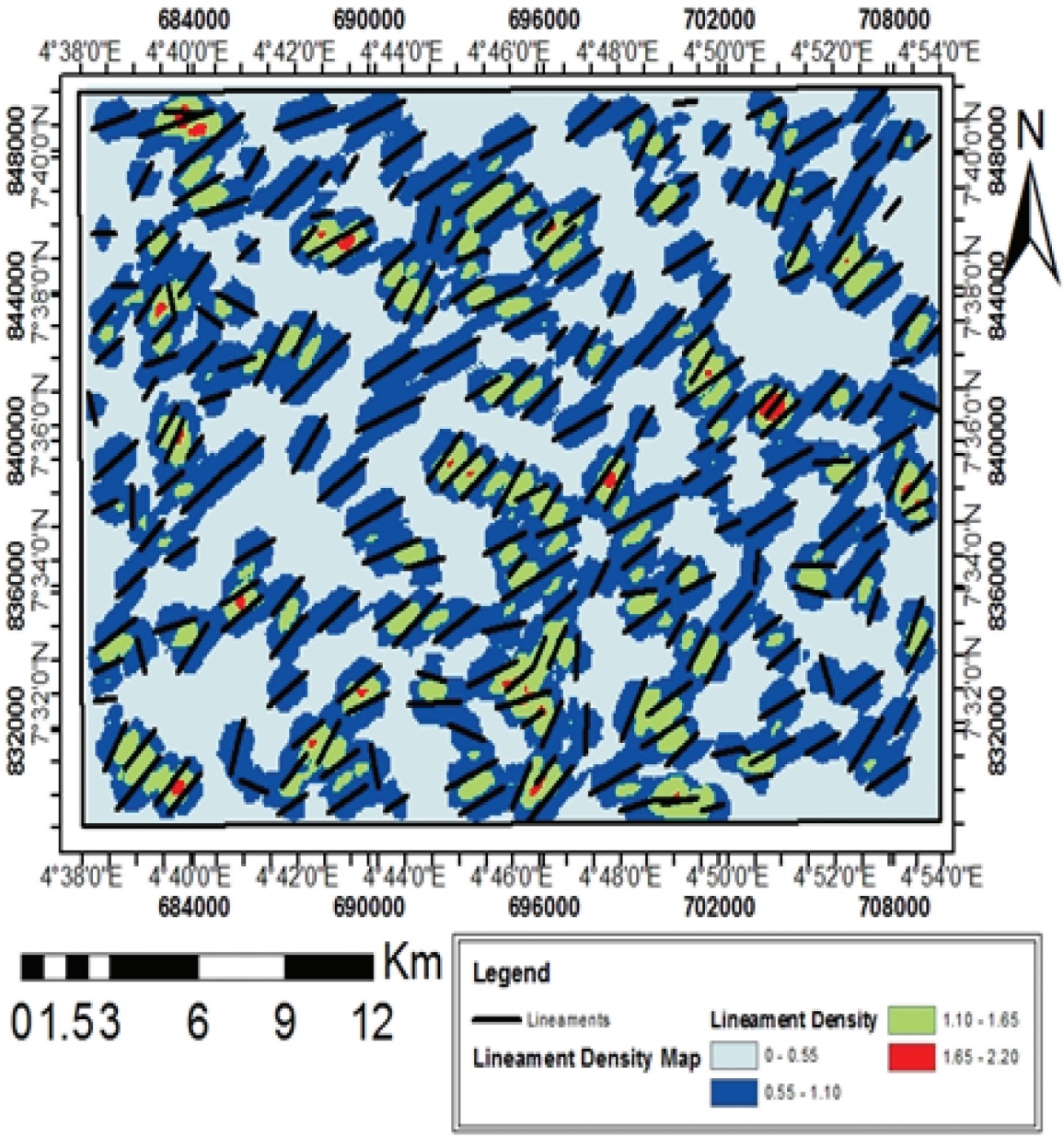

Figure 10. Composite aeromagnetic lineament density map.

correlation. The map showing the correlation was generated and is presented in Figure 13. Figure 13 was used to delineate areas that are considered to be more favourable for mineralisation in the investigated area. Magnetic low as observed on the RTE map, K high and KD anomalous high all define hydrothermally altered zones along several lithologies and their boundaries. These were carefully taken into account in generation of the relationship between magnetic lineament and alteration zones.

Figure 13 was validated by posting the existing gold mining pits on the map and is presented in Figure 14. From Figure 14, the region of high possibility of mineralisation are found to occupy the southern, middle and western parts of the study area. These are the regions where there is good correlation between the known mineralisation sites and the alteration zones. Therefore, this analysis showed that the structurally controlled mineralogical components in the study area adjudged the presence of hydrothermal alteration zones significantly associated with potassium enrichment.

5. Conclusions

Spatial relationships between alteration zones and mesothermal gold mineralisation were mapped using airborne geophysical datasets comprising magnetic and radiometry methods. The structural presentations

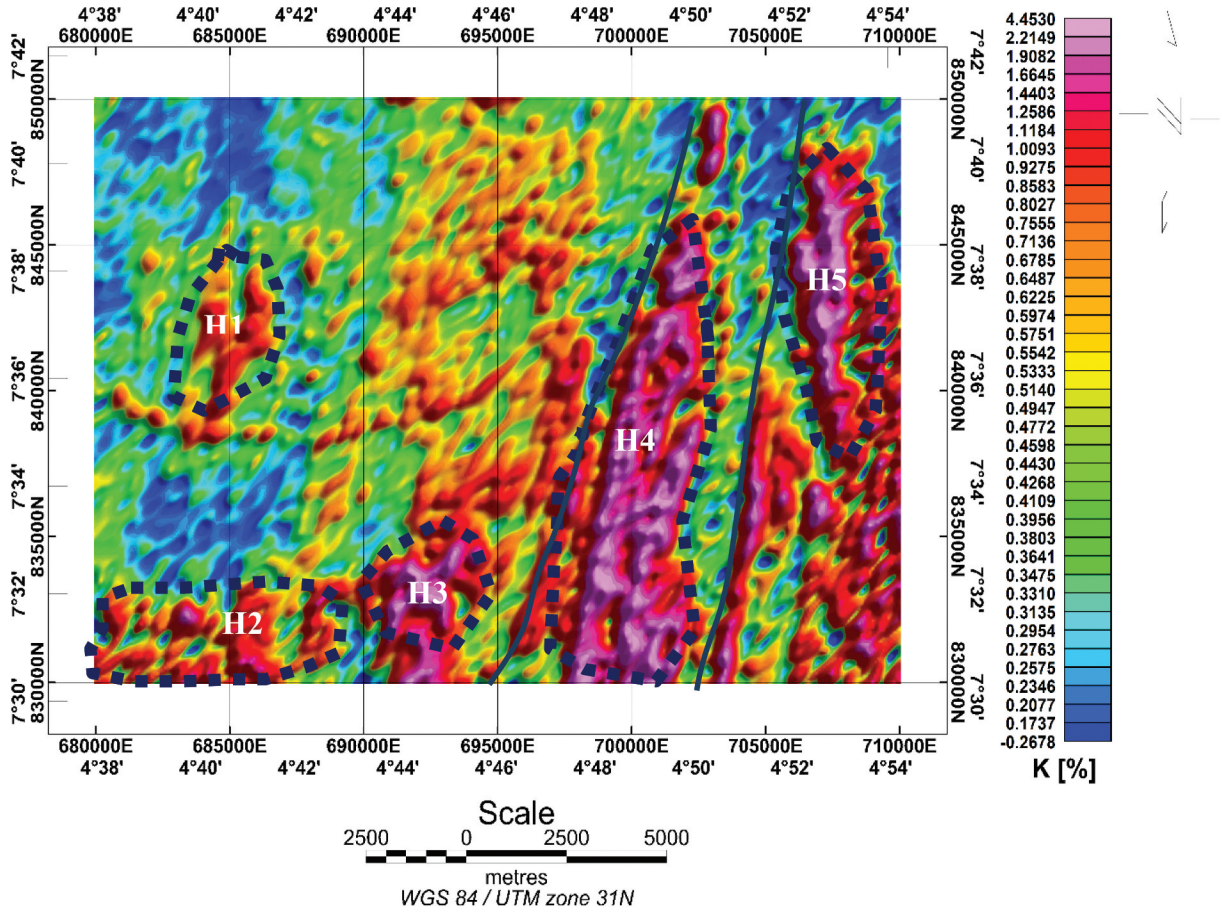

Figure 11. Potassium concentration map of the study area.

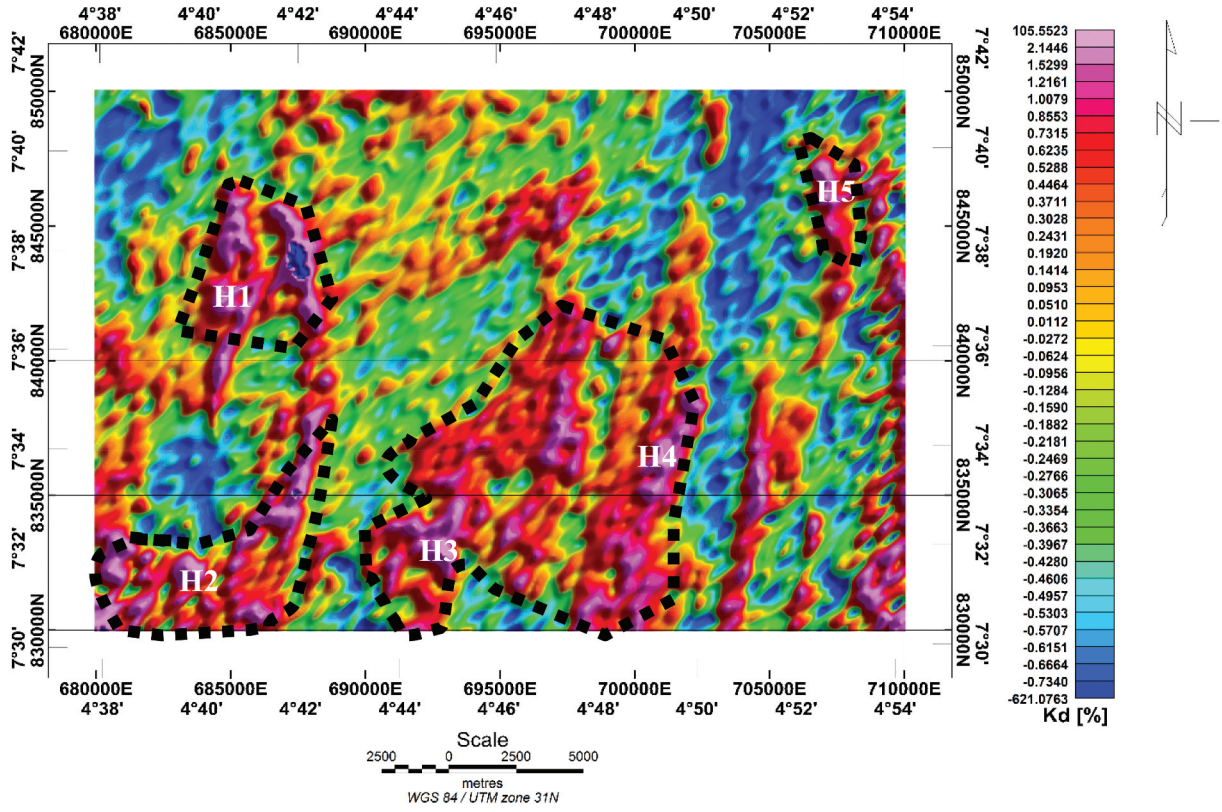

Figure 12. Potassium deviation map for hydrothermal zones delineation.

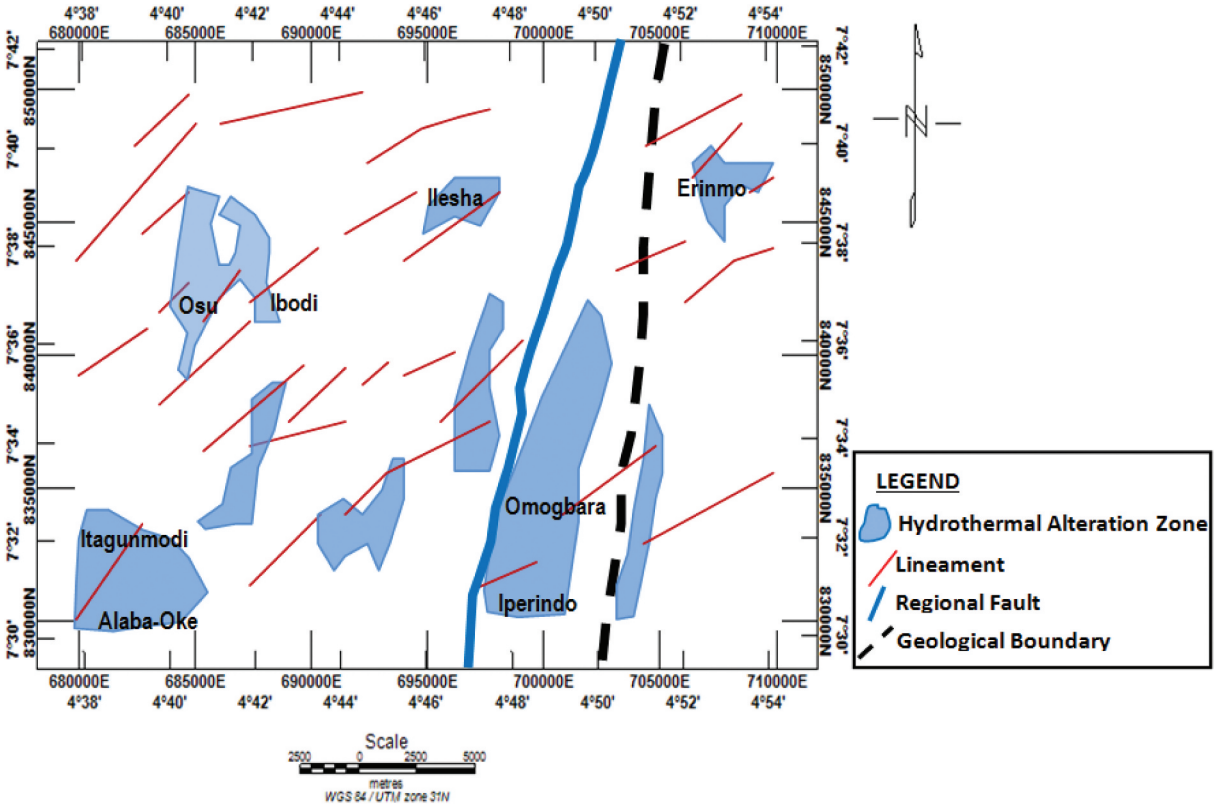

Figure 13. Relationship between magnetic lineament and hydrothermal alteration zones.

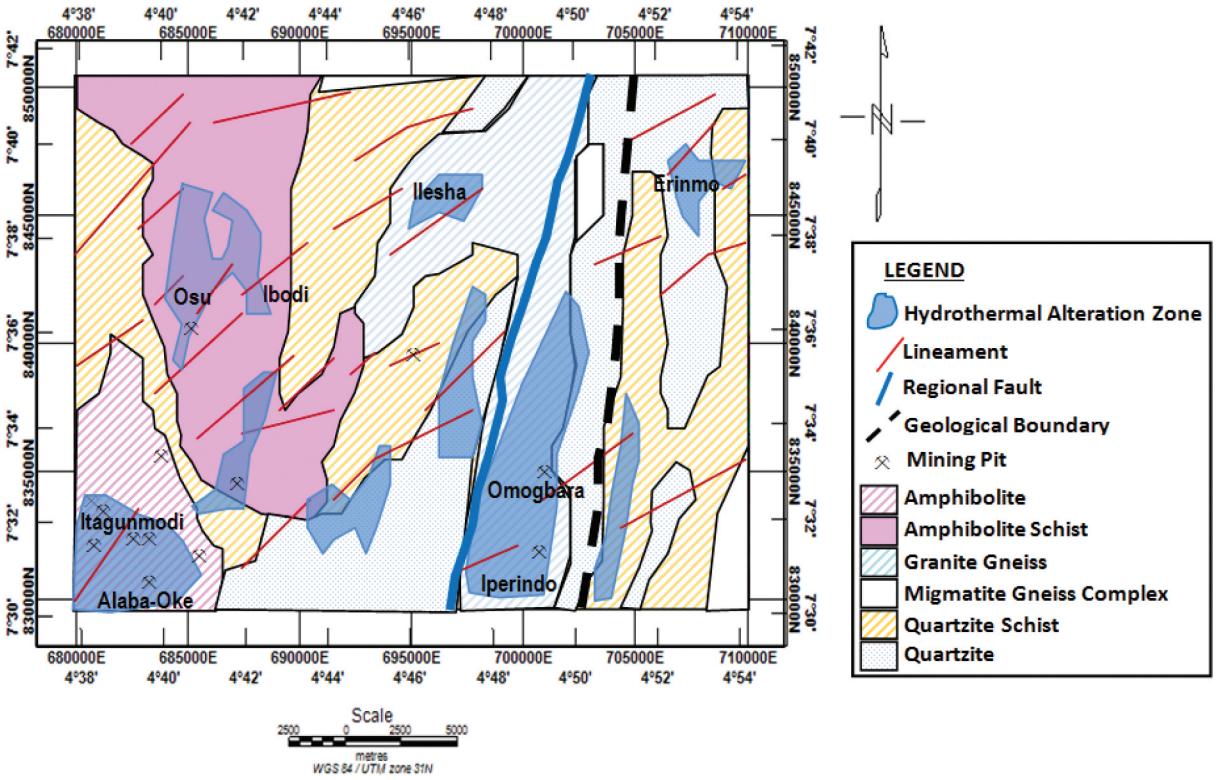

Figure 14. Predictive mineralisation map of the study area.

from the enhanced aeromagnetic data indicate shear zone, faults and fracture as magnetic anomalies that predominantly trend NW-SE and NE-SW directions. Airborne radiometry data processing reveals areas of alteration zones associated with potassium enrichment. These alteration zones were enhanced with the potassium deviation algorithm to give the real value of potassium concentration. Integration of the mapped lineaments and alteration zones delineated assisted in isolating/mapping areas of probable mineral deposit and subsequently produced the mineralisation predictive map of the study area. Verification of the predictive map was done using known existing gold mining pits sites present in the western part of Ilesha schist belt, southwestern part of Nigeria.

Disclosure statement

No potential conflict of interest was reported by the author(s).

ORCID

Kazeem Oladimeji Olomo http://orcid.org/0000-0001-5678-6661

References

Adams JAS, Gasparini P. (1970). Gamma ray spectrometry of rocks: elselvier Publ Co. New York, 295.

Adelusi AO, Adiat KAN, Amigun JO. 2009. Integration of Surface Electrical Prospecting Methods for Fracture Detection in Precambrian Basement Rocks of Iwaraja Area, Southwestern Nigeria. Journal of Mining and Geology. 18: 135–144.

Adelusi AO, Kayode JS, Akinlalu AA. 2013. Interpretation of aeromagnetic and electrical resistivity mapping around Iwaraja area, Southwestern Nigeria. J. Geol. Min. Res. 5 (2): 38–57.

Ademeso OA, Adekoya JA, Adetunji A. 2013. Further evidence of cataclasis in the ife-ilesa schist belt southwestern Nigeria. J Nat Sci Res. 3(11):50–59.

Adeoti B, Okonkwo CT. 2017. Structural evolution of Iwaraja shear zone, southwestern Nigeria. J Afr Earth Sci. 131:117–127. doi:10.1016/j.jafrearsci.2017.04.008.

Airo ML. 1997. Magnetic classification characterizing different types of early proterozoic metamorphosed black shales in Finland. In: Papunen H, editor. Mineral deposits. Vol. 4, Balkema (Rotterdam); Routledge & CRC Press Balkema, p. 33–35.

Airo ML, Mertanen S. 2008. Magnetic signatures related to orogenic gold mineralization, Central Lapland Greenstone Belt, Finland. J Appl Geophys. 64(1):14–24. doi:10.1016/j.jappgeo.2007.10.003.

Ajibade AC, (1979). The Nigerian precambrian and the Pan-African orogeny. In: Oluyide PO (Ed.), Proceedings of the first symposium on the Precambrian Geology of Nigeria, Geologic Survey of Nigeria., pp. 45–53.

Ajibade AC. 1982. The cataclastic rocks of the Zungeru region and tectonic significance. J Min Geol. 18:29–41.

Ajibade AC, Fitches WR. 1988. The Nigerian Precambrian and Pan-Africa Orogeny. [in:] Oluyide PO, Mbonu WC, Ogezi AEO, Egbuniwe IG, Ajibade AC and Umeji AC. (eds.), Precambrian Geology of Nigerian Geological Survey of Nigeria. 45–53.

Akande SO, Fakorede O. 1988. Gold mineralization in the Nigerian Schist Belts, Melbourne: Bicentennial Gold. 88: 140–152.

Akinlalu AA, Adelusi AO, Mamukuyomi EA, Akeredolu BE. 2016. Ground magnetic and 2-D resistivity mapping of basement structures around Iwaraja area southwestern Nigeria. J. Basic Appl. Res. Int. 18 (4): 206–221.

Akinlalu AA, Adelusi AO, Olayanju GM, Adiat KAN, Omosuyi GO, Anifowose AYB, Akeredolu BE. 2018. Aeromagnetic mapping of basement structures and mineralization characterisation of Ilesa schist belt, Southwestern Nigeria. J Afr Earth Sci. 138:383–391. doi:10.1016/j.jafrearsci.2017.11.033.

Ako BD. 1980. A contribution to mineral exploration in the Precambrian belt of part of southwestern Nigeria. Journal of Mining and Geology. 17(2): 129–138.

Anifowose AYB, Borode AM. 2007. A Photogeological study of the fold structure in Okemesi area. Niger J Min Geol. 43(2):125–130.

Araújo ILM, Dantas RAV, Vidotti EL, Fuck, R.A RM, Fuck RA. 2014. Tectonic framework of the São José do campestre massif, borborema province, based on new aeromagnetic data. Rev Bras Geofís. 32(3):445–463. doi:10.22564/rbgf.v32i3.502.

Ariyibi EA. 2011. Integrated Geochemical and Geophysical Approach to Mineral Prospecting – A Case Study on the Basement Complex of Ilesa Area, Nigeria, Advances in Data, Methods, Models and Their Applications in Geoscience, Dr. DongMei Chen (Ed.), ISBN: 978-953-307-737-6, InTech, Available from: http://www.intechopen.com/books/advances-in-data-methods-models-and-their-applications-ingeoscience/integrated-geochemical-and-geophysical-approach-to-mineral-prospecting-a-case-study-on-thebasement

Barbuena D, Souza Filho CR, Leite EP, Miguel E Jr., Assis RR, Xavier RP, Ferreira FJF, Paes de Barros AJ. 2013. Airborne geophysical data analysis applied to geological interpretation in the alta floresta gold province, MT. Rev Bras Geofís. 31(1):169–186. doi:10.22564/rbgf.v31i1.254.

Boesse TN, Ocan OO, (1988). Geology and Evolution of the Ife-Ilesha Schist Belt Southwestern Nigeria. In Benin-Nigeria Geotraverse. International Meeting on the Proterozoic Geology and Tectonics of High Grade Terrain. IGCP 215: 123-129

Burke KC, Freeth SJ, Grant NK. 1976. The structure and sequence of geological event in the basement complex of Ibadan area western Nigeria. Precamb Res. 3(6):537–545. doi:10.1016/0301-9268(76)90017-6.

Cooper GRJ, Cowan DR. 2006. Enhancing potential field data using filters based on the local phase. Comput Geosci. 32(10):1585–1591. doi:10.1016/j.cageo.2006.02.016.

Cordell L, Gruch VJS. 1985. 16. Mapping Basement Magnetization Zones from Aeromagnetic Data in the San Juan Basin, New Mexico, General Series: 181-197. https;//doi.org/10.1190/1.0931830346.ch16

De Quadros TFP, Koppe JC, Strieder AJ, Costa JFCL. 2003. Gamma-ray data processing and integration for lode-Au deposits exploration. Nat Resour Res. 12(1):57–65. doi:10.1023/A:1022608505873.

De Swart AMJ. 1953. The geology of the country around Ilesha. Geological survey of Nigeria. Bulletin. 23:154.

Dickson BL, Scott KM. 1997. Interpretation of aerial gamma-ray surveys—adding the geochemical factors: AGSO Jour. Australian Geology & Geophysics. 17 (2):187–200.

Ekwueme BN, Matheis G. 1995. Geochemistry and economic value of pegmatites in the Precambrian basement of southeastern Nigeria. New Delhi: Oxford & IBH Publishing Company.

Elueze AA. 1986. Petrology and gold mineralization of the amphibolites belt. Ilesa area southwestern Nigeria. Geo Mijnb. 65:189–195.

Ferreira FJF, Fornazzari-Neto L, Szameitat LSA, Guimarães GB, Martin VMO, Prazeres-Filho H, Ulbrich HH. 2014. Gamma-ray spectrometry as a tool for mapping petrographic domains in granitoids: the examples of the cunhaporanga and três córregos granitic complexes. Paraná State, Southern Brazil Rev Bras Geofís. 32(3):465–479.

Folami SL. 1992. Interpretation of aero magnetic anomalies in Iwaraja area, Southwestern Nigeria. J. Min. Geol., 28(2): 391–396

Folami SL, Ojo JS. 1991. Gravity and magnetic investigations over marble deposits in the Igara area Bendel state. J. Min. Geol., 27(1): 49–54.

FSN (Federal Survey of Nigeria). 1964. Topographic map of Ilesha schist belt. Produced by Federal Survey of Nigeria, now refeered to as Nigerian Geological Survey of Agency (NGSA).

Galbraith JH, Saunders DF. 1983. Rock classification by characteristics of aerial gamma ray measurements. J of Geochemical Expl. 18(1):49–73. doi:10.1016/0375-6742(83)90080-8.

Gilbert D, Geldano A. 1985. A computer to perform transmissions of gravimetric and aeromagnetic surveys. Comput Geosci. 11(5):553–588. doi:10.1016/0098-3004(85)90086-X.

Gunn PJ, Minty BRS. Milligan, and PR. 1997. The airborne gamma-ray spectrometric response over arid Australian terrains. In: Gubins, A.G. (Ed.), Exploration 97: Fourth Decennial International Conference on Mineral Exploration, Proceedings, 97: 733–740.

Gunn PJ, Minty BRS, Milligan PR, (1997). The airborne gamma-ray spectrometric response over arid Australian terrains. In: Gubins AG (Ed.), Exploration 97: Fourth Decennial International Conference on Mineral Exploration, Proceedings, pp. 733–740.

Ho SE, Groves DI. 1987. Recent advances in understanding Precambrian gold deposits. Geology Department and University Extension. University of Western Australia Publication, 11-368.

Hoover DB, Pierce HA. 1990. Annotated bibliography of gamma-ray methods applied to gold exploration: u.S. Geol Survey Open-File Rept. 90–203:23.

Kayode JS. 2009. Vertical components of the ground magnetic study of Ijebu-jesa, Southwestern Nigeria. A paper presented at the International Association of Seismologist and Physics of the Earth Interior (IASPEI) 2009 conference at Cape Town, South Africa Jan. 10th- 16th.

Keating P, Pilkington M. 2004. Euler Deconvolution of the analytic signal and its application to magnetic interpretation. Geophys Prospect. 52(3):165–182. doi:10.1111/j.1365-2478.2004.00408.x.

Kolawole F, Anifowose AYB. 2011. Remote Sensing Analysis of a Dextral Discontinuity along Ifewara-Zungeru Area, Nigeria, West Africa. Indian Journal of Science and Technology. 4(1): 46–51.

Korhonen JV. 2005. Airborne magnetic method: special features and review on applications. Geol Surv Finl Special. 39:77–102.

Kuster D. 1990. Rare-metal pegmatites of wamba, Central Nigeria-their formation in relation to late, Pan-African granites. Mineral Deposita. 25(1):25–33. doi:10.1007/BF03326380.

Matheis G. 1990. Nigerian rare metal pegmatites and their lithological framework. Journ, Geol. 22:271–291.

Matheis G, Caen-Vachette M. 1983. Rb-Sr isotopic study of rare metal bearing and barren pegmatites in the Pan African reactivation zone of Nigeria. J Afr Earth Sci. 1:35–40.

Maurin JC, Lancelot JR. 1990. Structural setting and U-Pb dating of uranium mineralisation from the Northeastern part of Nigeria (Upper Benue Region). J Afr Earth Sci. 10:421–433. doi:10.1016/0899-5362(90)90095-V.

McCurry P. 1987. The Geology of the Precambrian to Lower Paleozoic rocks of Northern Nigeria, a Review Inc A, Kogbe (Ed.), Geology of Nigeria. Lagos, Elizabethan. Publishing Co. .

McCurry P, And. Wright JB. 1977. Geochemistry of calc-alkaline volcanics in northwestern Nigeria, and a possible Pan-African suture zone. Earth Planet Sci Lett. 37:90–96. doi:10.1016/0012-821X(77)90149-2.

McDonald AI (1986). An international symposium on the geology of gold. Proceedings of gold ' 86. Toronto, pp 517.

Miller HG, Singh V. 1994. Potential field tilt – a new concept for location of potential field sources. J Appl Geophys. 32 (2–3):213–217. doi:10.1016/0926-9851(94)90022-1.

Minty BRS. 1997. The fundamentals of airborne gamma-ray spectrometry. AGSO J Aust Geol Geophys. 17(2):39–50.

Murat RC. 1972. Stratigraphy and Paleogeography of the Cretaceous and Lower Tertiary of Southern Nigeria. T.F. J. Dessauvagie and Whiteman (Eds), African Geology, Ibadan University press, Nigeria. 251-266.

Nabighian MN. 1972. The analytic signal of two-dimensional magnetic bodies with polygonal cross-section: its properties and use for automated anomaly interpretation. Geophysics. 37(3):507–517. doi:10.1190/1.1440276.

Nabighian MN. 1974. Additional comments on the analytic signal of two-dimensional magnetic bodies with polygonal cross-section. Geophysics. 39(1):85–92. doi:10.1190/1.1440416.

Ndousa-Mbarga T, Fenmoue ANS, Manguelle-Dicoum E, Fairhead JD. 2012. Aeromagnetic data interpretation to locate buried faults in south-East Cameroon. Geophysica. 48(1–2):49–63.

Obaje NG. 2009. Geology and mineral resources of Nigeria. London: Springer Dordrecht.

Odeyemi IB. 1993. A comparative study of remote sensing images of the structure of okemesi fold belt, Nigeria. ITC J. 1:77–81.

Okonkwo CT, Adetunji A, Folorunso IO. 2014. "Microstructural and mineralogical evolution of the oke awon shear zone in the jebba area, southwestern Nigeria. Pac J Sci Technol. 15:335 344.

Onyedim GC, Ocan OO. 2009. Spatial periodicities of structural features of the basement complex of southwestern Nigeria deduced from auto-covariance and power spectra of aeromagnetic data. The pacific journal of science and Technology. Pac. J. Sci. Technol. 10(1):556–566.

Oskooi B, Abedi M. 2015. An airborne magnetometry study across Zagros collision zone along Ahvaz–Isfahan route in Iran. J Appl Geophys. 123:112–122. doi:10.1016/j.jappgeo.2015.10.001.

Oyinloye AO, (1992). Genesis of the Iperindo gold deposit, Ilesha schist belt, Southwestern Nigeria. Unpublished thesis of the University of Wales, Cardiff (U.K). pp. 1–267.

Oyinloye AO. 2002b. Geochemical characteristics of some granite gneisses in Ilesha area southwestern Nigeria: implication on evolution of Ilesha schist belt, southwestern Nigeria. Trends in Geochemistry India. 2:59–71.

Oyinloye AO. 2004a. Petrochemistry, pb isotope systematic and geotectonic setting of granite gneisses in Ilesha schist belt southwestern Nigeria. Global Jour Geol Sci. 2(1):1–13.

Oyinloye AO. 2006b. Metallogenesis of the lode gold deposits in Ilesha area of Southwestern Nigeria: inferences from lead isotope systematic, Pak. J Sci Ind Res. 49(11):1–11.

Oyinloye AO. 2007. Geology and geochemistry of some crystalline basement rocks in Ilesha area sourthwestern Nigeria: implications on provenance and evolution Pak. J Sci Ind Res. 50(4):223–231.

Oyinloye AO. 2011. Geology and Geotectonic Setting of the Basement Complex Rocks in South Western Nigeria: Implications on Provenance and Evolution, Earth and Environmental Sciences, Dr. Imran Ahmad Dar (Ed.), ISBN: 978-953-307-468-9, InTech, Available from: http://www.intechopen.com/books/earthand-environmental-sciences/geology-and-geotectonic-setting-of-the-basement-complex-rocks-in-southwestern-nigeria-implications

Rahaman MA, Ocan OO.1978. On relationship in the Precambrian migmatitic gneisses of Nigeria. J Min and Geol. 15(1):23-30.

Rajagopalan S. 2003. Analytical Signal vs reduction to pole: solutions for low magnetic latitudes. Expl Geo. 34:257–262. doi:10.1071/EG03257.

Reid AB, Allsop JM, Granser H, Millett AJ, Somerton IW. 1990. Magnetic interpretation in three dimensions using Euler deconvolution. Geophysics. 55:80–90. doi:10.1190/1.1442774.

Ribeiro VB, Mantovani MSM. 2016. Gamma spectrometric and magnetic interpretation of cabaçal copper deposit inMato grosso (Brazil): implications for hydrothermal fluids remobilization. J Appl Geophys. 135:223–231. doi:10.1016/j.jappgeo.2016.10.016.

Roest WR, Verhoef V, Pilkington M. 1992. Magnetic interpretation using the 3-D analytic signal. Geophysics. 57:116–125. doi:10.1190/1.1443174.

Segilola Technical report (2016). Updated resource estimate for the segilola gold deposit, Osun State, Nigeria for Thor Explorations Ltd. pp 23–27

Thomas MD, Harris JR. 2009. Geological significant of high resolution aeromagnetic and radiometric data in the of the naver andste. marie plutons,central British Columbia: an example remote predictive mapping (RPM). Can J Remote Sensing. 35:s32–s53. doi:10.5589/m10-003.

Thompson DT. 1982. EULDPH: a new technique for making computer-assisted depth estimates from magnetic data. Geophysics. 47:31–37. doi:10.1190/1.1441278.

Tourlière B, Perrin J, Le Berre P, Pasquet FJ. 2003. Use of airborne gamma-ray spectrometry for kaolin exploration. J Appl Geophys. 53(2):91–102. doi:10.1016/S0926-9851(03)00040-5.

Verduzco B, Fairhead JD, Grenn CM, Mackenzie C. 2004. New insights into magnetic derivatives for structural mapping. Lead Edge. 23(2):116–119. doi:10.1190/1.1651454.

Wijns C, Perez C, Kowalczyk P. 2005. Theta map: edge detection in magnetic data. Geophysics. 70(4):L39–L43. doi:10.1190/1.1988184.